

PAPER

# Spontaneous growth of the reconnection electric field during magnetic reconnection with a guide field: A theoretical model and particle-in-cell simulations<sup>\*</sup>

To cite this article: Kai Huang *et al* 2020 *Chinese Phys. B* **29** 075202

View the [article online](#) for updates and enhancements.

# Spontaneous growth of the reconnection electric field during magnetic reconnection with a guide field: A theoretical model and particle-in-cell simulations\*

Kai Huang(黄楷)<sup>1,2</sup>, Quan-Ming Lu(陆全明)<sup>1,2,†</sup>, Rong-Sheng Wang(王荣生)<sup>1,2</sup>, and Shui Wang(王水)<sup>1,2</sup>

<sup>1</sup>Key Laboratory of Geospace Environment, Chinese Academy of Sciences, Department of Geophysics and Planetary Science, University of Science and Technology of China, Hefei 230026, China

<sup>2</sup>CAS Center for Excellence in Comparative Planetology, Hefei 230026, China

(Received 11 February 2020; revised manuscript received 21 April 2020; accepted manuscript online 28 April 2020)

Reconnection electric field is a key element of magnetic reconnection. It quantifies the change of magnetic topology and the dissipation of magnetic energy. In this work, two-dimensional (2D) particle-in-cell (PIC) simulations are performed to study the growth of the reconnection electric field in the electron diffusion region (EDR) during magnetic reconnection with a guide field. At first, a seed electric field is produced due to the excitation of the tearing-mode instability. Then, the reconnection electric field in the EDR, which is dominated by the electron pressure tensor term, suffers a spontaneous growth stage and grows exponentially until it saturates. A theoretical model is also proposed to explain such a kind of growth. The reconnection electric field in the EDR is found to be directly proportional to the electron outflow speed. The time derivative of electron outflow speed is proportional to the reconnection electric field in the EDR because the outflow is formed after the inflow electrons are accelerated by the reconnection electric field in the EDR and then directed away along the outflow direction. This kind of reinforcing process at last leads to the exponential growth of the reconnection electric field in the EDR.

**Keywords:** magnetic reconnection, reconnection electric field, electron diffusion region, particle-in-cell simulation

**PACS:** 52.35.Vd, 52.65.Rr, 52.35.Py, 94.05.–a

**DOI:** 10.1088/1674-1056/ab8da0

## 1. Introduction

Magnetic reconnection provides a mechanism for mass transport and energy conversion in many plasma physical settings. It is generally considered to be responsible for solar flares<sup>[1]</sup> and coronal mass ejections<sup>[2]</sup> in the solar atmosphere, substorms in the earth's magnetotail,<sup>[3–6]</sup> injections of the solar wind mass and energy into the earth's magnetopause,<sup>[7,8]</sup> and disruptions in the laboratory experiments.<sup>[9,10]</sup> In these plasma environments, the mean free path of charged particles is usually very large; thus the classical Coulomb collision is negligible. A collisionless reconnection model is believed to be suitable in these plasma systems.<sup>[11,12]</sup>

The reconnection electric field plays a pivotal role in both energy conversion and production of energetic particles during magnetic reconnection by doing work on particles.<sup>[13–17]</sup> In steady-state reconnection, the normalized reconnection electric field can be employed to represent the reconnection rate, and it is equivalent to the ratio of the inflow speed to the Alfvén speed. In collisionless magnetic reconnection, the diffusion region has two layers: the ion diffusion region and the electron diffusion region. In the electron diffusion region (EDR), both electrons and ions are unmagnetized, and electrons be-

come magnetized in the ion diffusion region. The reconnection rate in collisionless magnetic reconnection is mediated by the Hall effect resulting from such a kind of decoupled motions between ions and electrons, and the reconnection rate is around 0.1. Correspondingly, the reconnection electric field is about  $0.1v_A B_0$ , where  $v_A$  is the Alfvén speed, and  $B_0$  is the upstream magnetic field.<sup>[11,18]</sup> However, in reality, magnetic reconnection is non-stationary and the reconnection electric field is time evolutionary. The evolution of the reconnection electric field has three stages. A seed electric field is firstly produced in the current sheet, and then it grows until a maximum value is attained; finally its evolution saturates. The seed electric field can be generated by instabilities in the current sheet, such as the tearing-mode instability,<sup>[19–21]</sup> lower hybrid drift instability,<sup>[22,23]</sup> Buneman instability,<sup>[24,25]</sup> and Kelvin–Helmholtz instability.<sup>[26]</sup> In simulations of magnetic reconnection, the seed electric field is usually provided by an initial perturbation in order to bypass the linear growth of instabilities in the current sheet and forces the system into the reconnection stage, where the reconnection electric field grows spontaneously, from the beginning of the simulations.<sup>[11,13,27]</sup> When the initial perturbation is sufficiently small, it will not change

\*Project supported by the National Natural Science of China (Grant Nos. 41527804 and 41774169), the Strategic Priority Research Program of the Chinese Academy of Sciences (Grant No. XDB 41000000), and the Key Research Program of Frontier Sciences of the Chinese Academy of Sciences (Grant No. QYZDJ-SSW-DQC010).

†Corresponding author. E-mail: [qmlu@ustc.edu.cn](mailto:qmlu@ustc.edu.cn)

the following evolution of the reconnection electric field.<sup>[11]</sup>

Litvinenko<sup>[28]</sup> studied steady magnetic reconnection in the framework of incompressible Hall magnetohydrodynamics, they find that the Hall effect plays an important role in the reconnection rate enhancement and the current sheet thinning, and obtain an analytical relation between the reconnection electric field and the outflow speed. In collisionless magnetic reconnection, the reconnection electric field in the EDR is dominated by the divergence of the electron pressure tensor.<sup>[21,27]</sup> Hesse<sup>[29]</sup> further found that the reconnection electric field in the EDR is related to the gradient of the electron bulk velocity. However, so far, there were very few studies on the spontaneous growth of the reconnection electric field from the seed electric field in magnetic reconnection. Lu *et al.*<sup>[21]</sup> developed a theoretical model to explain the self-reinforcing process of the reconnection electric field in the EDR during anti-parallel magnetic reconnection. In the model, they proposed that the reconnection electric field is proportional to the electron outflow speed, while the electrons obtain their outflow speed from the acceleration by the reconnection electric field in the EDR. Such a self-reinforcing process leads to exponential growth of the reconnection electric field, which was further verified by two-dimensional (2D) particle-in-cell (PIC) simulations. Compared with anti-parallel reconnection, the more general case is guide field reconnection, where the shear angle between the reconnecting magnetic field cross the current sheet is less than  $180^\circ$ .<sup>[30]</sup> Previous studies indicated that the reconnection rate in guide field reconnection is only a little smaller than that in anti-parallel reconnection. However, the tearing-mode instability in the current sheet with a guide field and the structure of the diffusion region in guide field reconnection are greatly different from the anti-parallel case.<sup>[27,31]</sup> Therefore, in the present paper we will investigate the spontaneous growth of the reconnection electric field in the EDR during guide field reconnection.

## 2. Results from 2D PIC simulations

In this section, 2D PIC simulations are performed to investigate the evolution of the reconnection electric field during magnetic reconnection with a guide field. The simulation code has been successfully used to study magnetic reconnection and plasma waves.<sup>[13,32–36]</sup> The simulations are conducted in the  $x$ - $z$  plane, and the initial condition is the Harris-type current sheet with the magnetic field  $\mathbf{B}(z) = B_0 \tanh(z/\delta) \mathbf{e}_x - B_g \mathbf{e}_y$ , where  $B_g = B_0$  is a uniform guide field. The density profile is  $n(z) = n_0 \text{sech}^2(z/\delta) + n_b$ , where  $n_b = 0.2n_0$  is the background plasma density. The half width of the current sheet is  $\delta = 0.5d_i$ , where  $d_i$  is the ion inertial length based

on  $n_0$ . The initial velocity distributions of ions and electrons are assumed to be Maxwellian with the temperature ratio  $T_i/T_e = 4$ , and the ion-to-electron mass ratio is set to be  $m_i/m_e = 64$ . The speed of light is assumed to be  $c/v_A = 15$ , where  $v_A$  is the Alfvén speed based on  $B_0$  and  $n_0$ . The simulation domain is  $[-L_x, L_x] \times [-L_z, L_z]$  with spatial resolution  $\Delta x = \Delta z = 0.025d_i$ , where  $L_x = 30d_i$  and  $L_z = 7.5d_i$ . The time step is  $\Delta t = 0.001\Omega_i^{-1}$ , where  $\Omega_i$  is the ion gyrofrequency based on  $B_0$ . Nearly  $10^9$  computational particles per species are employed in the simulations. The periodic boundary condition is used in the  $x$  direction, while in the  $z$  direction the conducting boundary is assumed. In this paper, we at first run one case without an initial perturbation, and then investigate the influence of an initial perturbation on the evolution of the reconnection electric field. The form of the initial perturbation of the magnetic flux is expressed as  $\Delta\Psi = \Psi_0 \text{sech}^2(x/4\delta) \text{sech}^2(z/\delta)$ . Here, magnetic flux function  $\Psi$  satisfies  $\partial\Psi/\partial z = B_x$  and  $\partial\Psi/\partial x = -B_z$ .

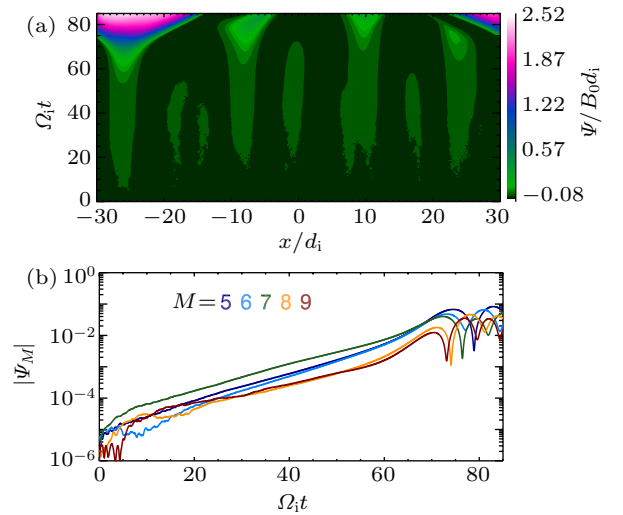


**Fig. 1.** (a) Time evolution of the magnetic flux function  $\Psi/(B_0 d_i)$  along  $z = 0$ . (b) Time evolution of  $|\Psi_M|$  with  $M = 5-9$ . In this case, there is no initial perturbation.

In the first case, we do not add any initial perturbation, or  $\Psi_0 = 0$ . The process of magnetic reconnection is clearly demonstrated in Fig. 1(a), which shows the magnetic flux  $\Psi/(B_0 d_i)$  along the line  $z = 0$  at different times. Figure 1(b) plots the time evolution of  $|\Psi_M|$  with different  $M$  calculated by the FFT of  $\Psi$ , where  $M = L_x k_x / \pi$ , and  $k_x$  is the wave number. Obviously, the current sheet is unstable to the tearing-mode instability, and the most unstable mode is  $M = 7$  mode, corresponding to  $k_x \delta = 0.37$ . It is in agreement with previous linear theory,<sup>[31]</sup> where  $k_x \delta = 0.3-0.5$  for the most unstable mode. At about  $\Omega_i t = 60$ , the magnetic flux  $\Psi$  around  $x = -26d_i$  increases rapidly, and reconnection begins to occur. Unlike other simulations of magnetic reconnection,<sup>[11,13]</sup> where an initial perturbation is added to bypass the excitation of the tearing-mode in the current sheet, in our simulations we

can observe the occurrence of magnetic reconnection following the tearing-mode instability.

In this paper, we focus on the spontaneous growth of the reconnection electric field after reconnection onset occurs. Figure 2 shows the time evolution of the electric field in the  $y$  direction  $E_y/v_A B_0$  (left panel) and electron current density in the  $y$  direction  $J_{ey}/en_0 v_A$  (right panel) with in-plane magnetic field lines for the case without an initial perturbation, panels (a)–(d) are displayed at  $\Omega_i t = 50, 60, 65,$  and  $70$ , respectively. Reconnection occurs around  $\Omega_i t = 60$ , and at that time both  $E_y$  and  $J_{ey}$  begin to be generated around the  $X$  line. As reconnection proceeds, the amplitude of both  $E_y$  and  $J_{ey}$  increases. During such a process, the electrons are accelerated by the reconnection electric field around the  $X$  line, and a thin electron current sheet embedded in the background current sheet is then formed. However, due to the deflection of the electron outflow by the guide field, the electron current sheet is biased along the lower left and upper right branches of the separatrices (the outflow separatrices) out of the EDR. This is consistent with previous studies.<sup>[15,27]</sup> The peak of the reconnection electric field is firstly located around the  $X$  line, and it gradually moves to the pile-up region, where the magnetic flux is accumulated by the high-speed electron flow away from the  $X$  line.<sup>[21]</sup>

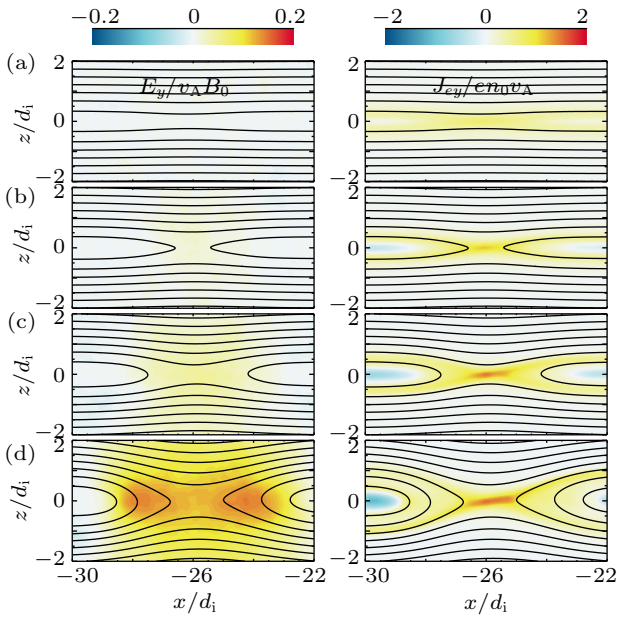


**Fig. 2.** The out-of-plane electric field  $E_y/v_A B_0$  and electron current density  $J_{ey}/en_0 v_A$  at  $\Omega_i t = 50$  (a),  $60$  (b),  $65$  (c), and  $70$  (d) respectively. Black curves show the in-plane magnetic field lines, and there is no initial perturbation in this case.

Using the electron momentum equation, one can easily find that the electric field can be expressed as

$$\mathbf{E} = -\mathbf{V}_e \times \mathbf{B} - \frac{\nabla \cdot \mathbf{P}_e}{en_e} - \frac{m_e}{e} \frac{d\mathbf{V}_e}{dt}, \quad (1)$$

where  $\mathbf{V}_e$  is the electron bulk velocity,  $n_e$  is the electron number density, and  $\mathbf{P}_e$  is the electron pressure tensor. Then, the

reconnection electric field  $E_y$  in the 2D condition ( $\partial/\partial y = 0$ ) can be written in the following expression

$$E_y = -(V_{ez}B_x - V_{ex}B_z) - \frac{1}{ene} \left( \frac{\partial P_{exy}}{\partial x} + \frac{\partial P_{eyz}}{\partial z} \right) - \frac{m_e}{e} \left( \frac{\partial V_{ey}}{\partial t} + V_{ex} \frac{\partial V_{ey}}{\partial x} + V_{ez} \frac{\partial V_{ey}}{\partial z} \right). \quad (2)$$

The three terms on the right-hand side are the electron convection term, electron pressure tensor term, and electron inertial term respectively.

After knowing the position and velocity of each particle, we can easily calculate the electron bulk velocity and electron pressure tensor. At last, we obtain the electron convection term, electron pressure tensor term, and electron inertial term as described in Eq. (2). Figure 3 shows the time evolution of the reconnection electric field  $E_y$  and its three decomposed terms along  $z = 0$  for the case without an initial perturbation. Obviously, the reconnection electric field in the EDR is dominated by the electron pressure tensor term, although both the electron convection and electron inertial terms are important outside the EDR. Also, the reconnection electric field and its three decomposed terms increase with the proceeding of magnetic reconnection, and they saturate at about  $\Omega_i t = 70$ .

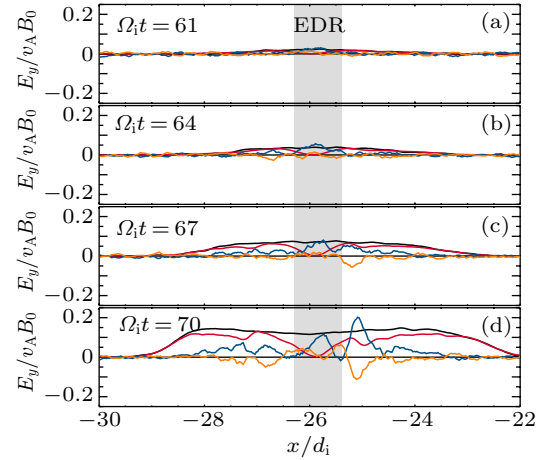


**Fig. 3.** Time evolution of the horizontal cut along  $z = 0$  of out-of-plane electric field  $E_y/v_A B_0$  (the black lines), electron convection term (the red lines), electron pressure tensor term (the blue lines), and electron inertial term (the orange lines) at  $\Omega_i t = 61$  (a),  $64$  (b),  $67$  (c), and  $70$  (d). Electron diffusion region is denoted by gray color. In this case, there is no initial perturbation.

In general, the reconnection electric field at the  $X$  line is used to quantify the topological change of magnetic field lines, and it is also related to the conversion of magnetic energy into plasma kinetic energy and the production of energetic particles. Therefore, in this paper, we focus on the evolution of the reconnection electric field at the  $X$  line, or its self-reinforcing process, during magnetic reconnection. Figure 4 plots the time evolution of the reconnection electric field  $E_y$  at the  $X$  line for the case without an initial perturbation. The reconnection electric field grows exponentially at about  $\Omega_i t = 60$ , and saturates

at about  $\Omega_i t = 70$ . The growth rate is estimated to be about  $0.226\Omega_i$ .

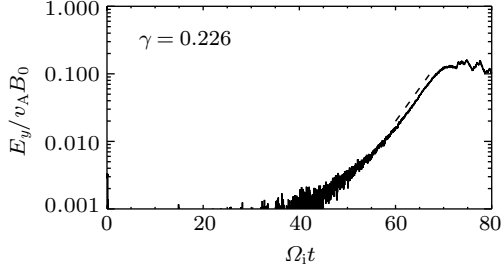


**Fig. 4.** Time evolution of the out-of-plane electric field  $E_y/v_A B_0$  in the EDR. The dashed line shows the fitted exponential growth rate. In this case, there is no initial perturbation.

We also run two cases with initial perturbations, whose amplitudes of the magnetic flux are  $\Psi_0/(B_0 d_i) = 0.05$  and  $0.1$ , respectively. The evolution of the reconnection electric field  $E_y$  at the  $X$  line in these simulations is plotted in Fig. 5. Compared to the case without an initial perturbation, magnetic reconnection occurs much earlier when an initial perturbation is introduced. However, in all these cases the reconnection electric field follows an exponential growth later (from  $\Omega_i t = 10$  to  $20$  and  $10$  to  $15$  when the amplitude of the initial perturbation is  $\Psi_0/(B_0 d_i) = 0.05$  and  $0.1$ , respectively), and the growth rate is almost the same. In the case without an initial perturbation, the growth rate is about  $0.226\Omega_i$ , while it is about  $0.225\Omega_i$  and  $0.236\Omega_i$  when the amplitude of the initial perturbation is  $\Psi_0/(B_0 d_i) = 0.05$  and  $0.1$ , respectively. Therefore, the spontaneous growth of the reconnection electric field, which is the focus in this paper, is not affected by the initial perturbation with small amplitude.

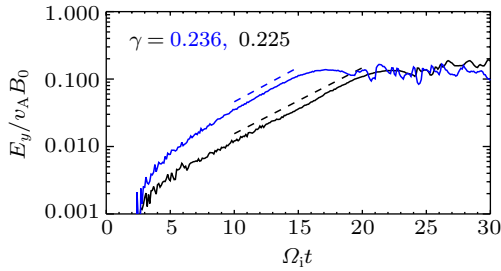


**Fig. 5.** Time evolution of the reconnection electric field  $E_y/v_A B_0$  when the initial perturbation amplitude is  $\Psi_0/(B_0 d_i) = 0.05$  (the black line) and  $0.1$  (the blue line) respectively. The dashed lines show the fitted growth rate.

### 3. Theoretical model

A theoretical model is proposed in this section to describe the spontaneous growth of the reconnection electric field in the EDR during guide field reconnection. From the simulation, we see that the reconnection electric field around the  $X$  line is mainly balanced by the electron pressure tensor term, and it can be expressed as<sup>[29]</sup>

$$E_y \approx \frac{r_L^2}{2en_e} \frac{\partial V_{ex}}{\partial x} \nabla^2 (m_e n_e V_{ey}), \quad (3)$$

where  $r_L$  is the electron Larmor radius in the guide field,  $V_{ex}$  and  $V_{ey}$  are the electron bulk velocities in the  $x$  and  $y$  directions. When Hesse<sup>[29]</sup> obtain this equation, it is assumed that the overall evolution time scale of the reconnection electric field is related to the ion cyclotron period, and the current density does not change with time. From our simulations, we can find that these assumptions are reasonable. We also compare the evolution of the reconnection electric field directly obtained from the simulations with those calculated by Eq. (3), and find that they are consistent.

Figure 6 depicts the sketch of the EDR. Usually, the length of the EDR is much larger than its width. So  $\partial^2/\partial z^2 \gg \partial^2/\partial x^2$ . Combined with  $J_{ey} = -en_e V_{ey}$ , we get  $\nabla^2 (m_e n_e V_{ey}) \approx -(m_e/e) \partial^2 J_{ey}/\partial z^2$ . If we denote the half length and width of the EDR by  $L_e$  and  $\delta_e$ , respectively, the reconnection electric field around the  $X$  line can be approximated as

$$E_y \approx \frac{m_e r_L^2 J_{ey}}{2e^2 n_e L_e \delta_e^2} V_{e,out}, \quad (4)$$

where  $V_{e,out}$  is the electron outflow speed along the  $x$  direction at the edge of the EDR.

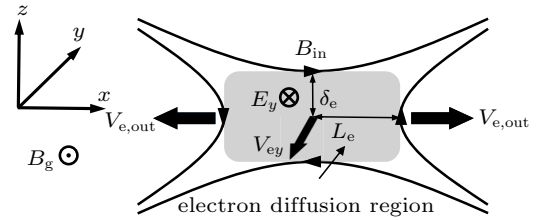


**Fig. 6.** A sketch of the electron diffusion region.<sup>[21]</sup>

If we assume that the EDR is stationary during the spontaneous growth of the reconnection electric field, the parameters  $J_{ey}$ ,  $\delta_e$ ,  $L_e$ ,  $n_e$ , and  $r_L$  are kept as constants. Then, from Eq. (4), we can know that the reconnection electric field is in direct proportion to the electron outflow speed

$$E_y \propto V_{e,out}. \quad (5)$$

The electrons move into the EDR from the inflow region and simultaneously get accelerated along the  $y$  direction by the reconnection electric field. At last, they leave the EDR and form electron outflows with the outflow speed  $V_{e,out}$  after they get a sufficiently large speed  $V_{ey}^0$ . Therefore,  $V_{e,out} \propto V_{ey}^0$ . Because in the EDR  $\partial V_{ey}^0/\partial t \propto E_y$ , we can obtain

$$\frac{\partial V_{e,out}}{\partial t} \propto E_y. \quad (6)$$

Combined with Eq. (5), the following equation can be obtained:

$$\frac{\partial E_y}{\partial t} \propto E_y. \quad (7)$$



Therefore, the reconnection electric field  $E_y$  around the  $X$  line will grow exponentially. If the growth rate is denoted by  $\gamma$ ,

$$E_y \propto e^{\gamma t}. \quad (8)$$

Also, the electron outflow speed along the  $x$  direction at the edge of the EDR ( $V_{e,\text{out}}$ ) grows exponentially with the same growth rate  $\gamma$ .

#### 4. Discussion

In our theoretical model, we assume that the half length and width of the EDR  $L_e$  and  $\delta_e$ , as well as the electron current density in the  $y$  direction  $J_{ey}$ , electron density  $n_e$ , and electron Larmor radius in the guide field  $r_L$  in the EDR are unchanged. Based on the simulations described in Section 2, we plot their time evolution in Fig. 7. Here,  $\delta_e$  is calculated by the half width of the electron current sheet along  $x = 0$  in the EDR.  $L_e$  is the half separation between the two peaks of the electron bulk velocity  $V_{ex}$  along  $z = 0$ , the average of the absolute value of the two peaks is defined as  $V_{e,\text{out}}$  (see Eq. (4)),  $r_L$  is the electron Larmor radius in the guide field defined as  $m_e v_{\text{the}\perp} / e |B_y|$  in the EDR, where  $v_{\text{the}\perp} = \sqrt{2T_{e\perp} / m_e}$ . Because an initial perturbation with small amplitude does not change the spontaneous growth of the reconnection electric field, the amplitude of the initial perturbation in this session is  $\Psi_0 / (B_0 d_i) = 0.05$ . During  $\Omega_i t = 10$  to  $\Omega_i t = 20$ , when the reconnection electric field grows exponentially,  $\delta_e$ ,  $L_e$ , and  $r_L$  are nearly constant; the variations of  $J_{ey}$  and  $n_e$  are also much smaller than  $E_y$ , which is increased by a factor of 10 (see Fig. 5). Therefore, the assumptions used in our theoretical model are reasonable.

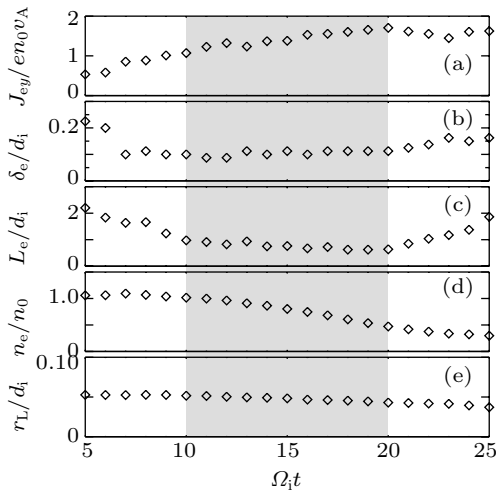


**Fig. 7.** Time evolution of (a) the  $y$  directional electron current density  $J_{ey} / en_0 v_A$  in the EDR, (b) the half width of EDR  $\delta_e / d_i$ , (c) the half length of EDR  $L_e / d_i$ , (d) the electron density  $n_e$  in the EDR, and (e) the electron Larmor radius in the guide field  $r_L$  in the EDR. The initial perturbation amplitude is  $\Psi_0 / (B_0 d_i) = 0.05$ .

To examine the robustness of the theoretical model, we vary the amplitude of the guide field to  $B_g / B_0 = 1, 2, \text{ and } 3$ .

The other parameters are kept fixed as those described in Section 2. As shown in Fig. 8, the evolution of the reconnection electric field is similar in the three cases, which exhibit the exponential growth phase presented before the reconnection rate reaches maximum. The time evolution of the electron outflow speed  $V_{e,\text{out}} / v_A$  is also plotted. During the growth phase of  $E_y$ ,  $V_{e,\text{out}}$  is approximately proportional to  $E_y$ , and grows exponentially with a growth rate a little smaller than that of  $E_y$ . The small difference between the growth rates of  $V_{e,\text{out}}$  and  $E_y$  should come from our assumption that  $J_{ey}$  and  $n_e$  are unchanged during this process. From Eq. (4) and Fig. 7 we can learn that the increase of  $J_{ey}$  and the decrease of  $n_e$  lead to a smaller growth rate of  $V_{e,\text{out}}$  than  $E_y$ . We also note that the growth rate of  $V_{e,\text{out}}$  decreases after around  $\Omega_i t = 12, 13, \text{ and } 15$  in Figs. 8(a)–8(c). Because the electron outflow is not strictly along  $z = 0$ , there will be an error when we measure the electron outflow speed, causing the discrepancy between the growth rate of  $V_{e,\text{out}}$  and  $E_y$ . In general, we can conclude that the proposed model is reasonable to explain the spontaneous growth of the reconnection electric field in the EDR during guide field reconnection.

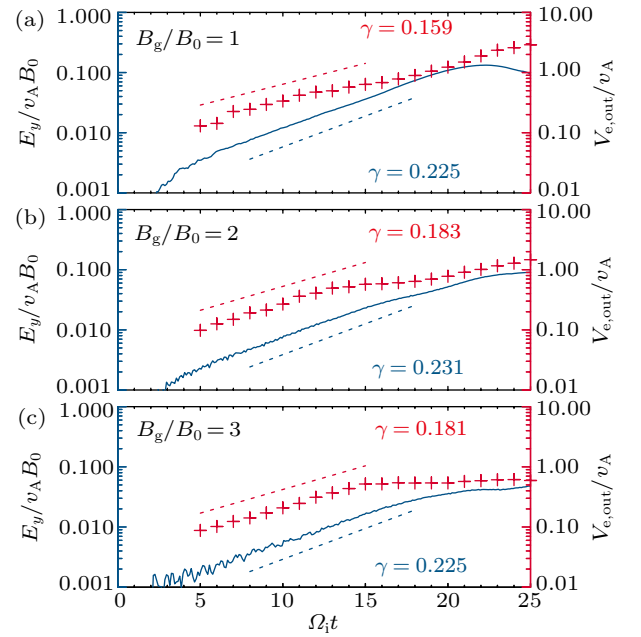


**Fig. 8.** Time evolution of the reconnection electric field  $E_y / v_A B_0$  (the blue line) and electron outflow speed  $V_{e,\text{out}} / v_A$  (the red cross) when the guide field is  $B_g / B_0 = 1, 2, \text{ and } 3$ . The growth rates of the reconnection electric field and electron outflow speed are also shown in each panel. The initial perturbation amplitude is  $\Psi_0 / (B_0 d_i) = 0.05$ .

#### 5. Conclusions

In this paper, based on both 2D PIC simulations and a proposed theoretical model, we have investigated the spontaneous growth of the reconnection electric field in the EDR during magnetic reconnection with a guide field. The reconnection electric field in the EDR is dominated by the electron pressure tensor term, while it is found to be directly proportional to the

electron outflow speed. The time derivative of electron outflow speed is proportional to the reconnection electric field in the EDR because the outflow is formed after the inflow electrons are accelerated by the reconnection electric field in the EDR and directed away along the outflow direction. This kind of reinforcing process at last leads to the exponential growth of the reconnection electric field in the EDR. In this paper, we do not consider the influence of secondary islands which may be formed in the EDR during the evolution of magnetic reconnection on the spontaneous growth of the reconnection electric field, and this is our future plan.

## References

- [1] Shibata K and Magara T 2011 *Living Rev. Sol. Phys.* **8** 1
- [2] Chen P F 2011 *Living Rev. Sol. Phys.* **8** 1
- [3] Sergeev V A, Angelopoulos V and Nakamura R 2012 *Geophys. Res. Lett.* **39** L05101
- [4] Pu Z Y, Chu X N, Cao X, Mishin V, Angelopoulos V, Wang J, Wei Y, Zong Q G, Fu S Y, Xie L, Glassmeier K H, Frey H, Russell C T, Liu J, McFadden J, Larson D, Mende S, Mann I, Sibeck D, Sapronova L A, Tolochko M V, Saifudinova T I, Yao Z H, Wang X G, Xiao C J, Zhou X Z, Reme H and Lucek E 2010 *J. Geophys. Res.-Space Phys.* **115** A02212
- [5] Fu H S, Cao J B, Cao D, Wang Z, Vaivads A, Khotyaintsev Y V, Burch J L and Huang S Y 2019 *Geophys. Res. Lett.* **46** 48
- [6] Angelopoulos V, McFadden J P, Larson D, Carlson C W, Mende S B, Frey H, Phan T, Sibeck D G, Glassmeier K H, Auster U, Donovan E, Mann I R, Rae I J, Russell C T, Runov A, Zhou X Z and Kepko L 2008 *Science* **321** 931
- [7] Le A, Daughton W, Chen L J and Egedal J 2017 *Geophys. Res. Lett.* **44** 2096
- [8] Nakamura T K M, Eriksson S, Hasegawa H, Zenitani S, Li W Y, Genestreti K J, Nakamura R and Daughton W 2017 *J. Geophys. Res.-Space Phys.* **122** 11505
- [9] Zelenyi L and Artemyev A 2013 *Space Sci. Rev.* **178** 441
- [10] Yu Q, Gunter S and Lackner K 2014 *Nucl. Fusion* **54** 072005
- [11] Birn J, Drake J F, Shay M A, Rogers B N, Denton R E, Hesse M, Kuznetsova M, Ma Z W, Bhattacharjee A, Otto A and Pritchett P L 2001 *J. Geophys. Res.-Space Phys.* **106** 3715
- [12] Zweibel E G and Yamada M 2009 *Ann. Rev. Astron. Astrophys.* **47** 291
- [13] Fu X R, Lu Q M and Wang S 2006 *Phys. Plasmas* **13** 012309
- [14] Hoshino M, Mukai T, Terasawa T and Shinohara I 2001 *J. Geophys. Res.-Space Phys.* **106** 25979
- [15] Huang C, Lu Q M and Wang S 2010 *Phys. Plasmas* **17** 072306
- [16] Lu Q M, Wang H Y, Huang K, Wang R S and Wang S 2018 *Phys. Plasmas* **25** 072126
- [17] Pritchett P L 2006 *Geophys. Res. Lett.* **33** L13104
- [18] Cassak P A, Liu Y H and Shay M A 2017 *J. Plasma Phys.* **83** 715830501
- [19] Biskamp D, Sagdeev R Z and Schindler K 1970 *Cosmic Electrodynamics* **1** 297–310
- [20] Galeev A A, Coroniti F V and Ashourabdalla M 1978 *Geophys. Res. Lett.* **5** 707
- [21] Lu Q M, Lu S, Huang C, Wu M Y and Wang S 2013 *Plasma Phys. Control. Fusion* **55** 085019
- [22] Daughton W 2003 *Phys. Plasmas* **10** 3103
- [23] Scholer M, Sidorenko I, Jaroschek C H, Treumann R A and Zeiler A 2003 *Phys. Plasmas* **10** 3521
- [24] Che H, Drake J F, Swisdak M and Yoon P H 2009 *Phys. Rev. Lett.* **102** 145004
- [25] Drake J F, Swisdak M, Cattell C, Shay M A, Rogers B N and Zeiler A 2003 *Science* **299** 873
- [26] Shinohara I, Suzuki H, Fujimoto M and Hoshino M 2001 *Phys. Rev. Lett.* **87** 095001
- [27] Pritchett P L 2001 *J. Geophys. Res.-Space Phys.* **106** 3783
- [28] Litvinenko Y E 2009 *Astrophys. J.* **694** 1464
- [29] Hesse M 2006 *Phys. Plasmas* **13** 122107
- [30] Lapenta G, Markidis S, Divin A, Goldman M and Newman D 2010 *Phys. Plasmas* **17** 082106
- [31] Daughton W and Karimabadi H 2005 *J. Geophys. Res.-Space Phys.* **110** A03217
- [32] Huang K, Lu Q M, Huang C, Dong Q L, Wang H Y, Fan F B, Sheng Z M, Wang S and Zhang J 2017 *Phys. Plasmas* **24** 102101
- [33] Ke Y G, Gao X L, Lu Q M and Wang S 2017 *Phys. Plasmas* **24** 012108
- [34] Lu S, Angelopoulos V and Fu H S 2016 *J. Geophys. Res.-Space Phys.* **121** 9483
- [35] Sang L L, Lu Q M, Wang R S, Huang K and Wang S 2018 *Phys. Plasmas* **25** 062120
- [36] Li Z S, Wang H Y and Gao X L 2019 *Chin. Phys. B* **28** 075203